

# Halogen Bonding in the Assembly of Coordination Polymers Based on 5-Iodo-Isophthalic Acid

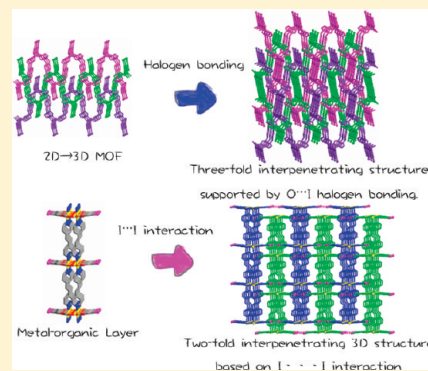
Shuang-Quan Zang,<sup>\*,†</sup> Ya-Juan Fan,<sup>†</sup> Jia-Bin Li,<sup>†</sup> Hong-Wei Hou,<sup>†</sup> and Thomas C. W. Mak<sup>†,‡</sup>

<sup>†</sup>Department of Chemistry, Zhengzhou University, Zhengzhou 450001, P. R. China

<sup>‡</sup>Department of Chemistry, The Chinese University of Hong Kong, Shatin, New Territories, Hong Kong SAR, P. R. China

Supporting Information

**ABSTRACT:** A series of seven divalent coordination polymers based on 5-iodoisophthalic acid (5-iipa) and ancillary nitrogen ligands (phen = 1,10-phenanthroline, bpe = 1,2-bis(4-pyridyl)ethene, *p*-bix = 1,4-bis(imidazol-1-ylmethyl)-benzene, *m*-bix = 1,3-bis(imidazol-1-ylmethyl)-benzene), namely,  $[Zn_2(5\text{-iipa})_2(\text{phen})_2(\text{H}_2\text{O})]_n$  (**1**),  $[Zn(5\text{-iipa})(\text{bpe})_{1.5}]_n$  (**2**),  $[\text{Cd}_2(5\text{-iipa})_2(\text{phen})_2]_n$  (**3**),  $[\text{Mn}_2(5\text{-iipa})_2(\text{phen})_2]_n$  (**4**),  $[\text{Mn}_4(5\text{-iipa})_4(\text{bpe})_4 \cdot 5\text{H}_2\text{O}]_n$  (**5**),  $[\text{Co}(5\text{-iipa})(\text{p-bix})]_n$  (**6**), and  $[\text{Co}(5\text{-iipa})(\text{m-bix})]_n$  (**7**), have been synthesized. The structure of compound **1** exhibits a double zigzag metal–organic chain, and such chains are further united together to generate a three-dimensional (3D) supramolecular structure through interchain  $\text{I} \cdots \pi$  interactions. Compound **2** features interesting 3-fold parallel interpenetrated two-dimensional (2D)  $\rightarrow$  3D network motifs which are stabilized by interlayer  $\text{I} \cdots \pi$ ,  $\pi \cdots \pi$ , and  $\text{C}-\text{H} \cdots \pi$  interactions. In isomorphous compounds **3** and **4**, the 5-iipa<sup>2-</sup> ligand acts as a  $\mu_3$ -bridge to connect metal atoms to form a 2D metal–organic layer, and such layers are united together to yield a 3D supramolecular structure through interlayer  $\text{I} \cdots \pi$  and  $\text{C}-\text{H} \cdots \pi$  interactions. In the structures of **5** and **7**, the rare 2-fold interpenetrating 3D supramolecular architectures based on  $\text{I} \cdots \text{I}$  interactions or  $\text{O} \cdots \text{I}$  halogen bonding are found, respectively. In compound **6**, 3-fold interpenetrated 2D  $\rightarrow$  3D network motifs based on covalent bonding are expanded to a rare 3D supramolecular structure based on  $\text{O} \cdots \text{I}$  halogen bonding. The above results demonstrate a useful guideline in the crystal engineering of supramolecular architectures in coordination network assembly under the influence of halogen bonding as well as related  $\text{I} \cdots \text{I}$  and  $\text{I} \cdots \pi$  interactions. Their thermal analysis, X-ray diffraction, UV-vis absorption spectra, and photoluminescent properties have been investigated as well.



## INTRODUCTION

Halogen bonding<sup>1</sup> ( $\text{D} \cdots \text{X}-\text{Y}$ ) in which X is the halogen (Lewis acid, halogen bonding donor), D is any donor of electron density (Lewis base, halogen bonding acceptor), and Y is carbon, nitrogen, halogen, etc., have been well appreciated in the past few years. Both  $\pi$  and  $n$  electrons can be involved in halogen bonding formation, and usually the former give weaker interactions than the latter. Halocarbons RX, where R is an alkyl or aryl group and X is a halogen atom, constitute a unique type of ligand in coordination chemistry owing to the potential formation of halogen bonding as well as related  $\text{I} \cdots \text{I}$  and  $\text{I} \cdots \pi$  interactions.<sup>2</sup> Metrangolo and Resnati<sup>1,3</sup> and other research groups<sup>2,4</sup> have demonstrated the effectiveness of such interactions in crystal engineering, thereby drawing widespread interest in many fields, most notably in connection with drug–receptor interactions,<sup>5</sup> halide–anion receptors,<sup>6</sup> supramolecular organic conductors,<sup>7</sup> liquid crystals,<sup>8</sup> crystal plasticity,<sup>9</sup> nonlinear optics (NLO),<sup>10</sup> luminescence,<sup>11</sup> and nanomaterials.<sup>12</sup> Remarkably, the halogen bonding exhibits characteristics comparable to the hydrogen bonding with regard to directionality and strength.<sup>13</sup>

Despite some successful achievements in the design of crystalline materials with interesting structural topologies and/or

properties, true crystal engineering<sup>14</sup> still remains a quite difficult and long-term challenge. As this area has developed, certain strategies have been widely exploited, most notably of which are metal coordination<sup>15,16</sup> and hydrogen bonding.<sup>17</sup> The tailored introduction and evaluation of noncovalent assembly in metal–organic frameworks is very important, now that the identification and summarization of such supramolecular synthons facilitate a better comprehension of the crystal structures for the systematic design of related materials. The role of hydrogen,<sup>18</sup>  $\pi \cdots \pi$ ,<sup>19</sup> and  $\text{C}-\text{H} \cdots \pi$ <sup>20</sup> bonding effects on assembly of metal–organic networks has been analyzed. The coexistence of halogen-related interactions in combination with metal coordination within a given crystalline compound, usually obtained accidentally, has been systematically summarized.<sup>21</sup> Attempted assembly of discrete coordination complexes using halogen bonding or halogen  $\cdots$  halogen interactions into one- or two-dimensional (1D or 2D) supramolecular structures has proven its difficulty.<sup>22,23</sup> The effect of halogen-related interactions in the

**Received:** January 8, 2011

**Revised:** May 20, 2011

**Published:** June 17, 2011

assembly of high-dimensional coordination polymers remains largely unexplored and needs more elaborate and systematic studies.<sup>24</sup>

To this end, we considered it worthwhile to make use of the rigid ligand 5-iodo-isophthalic acid (5-iipa),<sup>25</sup> which possesses two carboxylate groups for coordination to metal centers,<sup>26</sup> and its iodine atom is potentially capable of partaking in oxygen (or nitrogen)···I halogen bonding and related I···π and I···π interactions. Additionally, the use of auxiliary ligands is also an effective method for the construction of coordination polymers owing to the fact that they can mediate the coordination needs of the metal center and many metal–organic coordination polymers have been constructed from the “mix-ligand” synthetic strategies.<sup>27</sup> In our investigation of the coordination chemistry of 5-iodo-isophthalic acid, we have selected four nitrogen heterocyclic ligands as ancillaries, namely, phen, bpe, *p*-bix, and *m*-bix.

Here we report the synthesis and structure of a series of seven divalent metal 5-iipa coordination polymers that incorporate some selected N-containing auxiliary ligands: [Zn<sub>2</sub>(5-iipa)<sub>2</sub>(phen)<sub>2</sub>·(H<sub>2</sub>O)]<sub>n</sub> (**1**), [Zn(5-iipa)(bpe)<sub>1.5</sub>]<sub>n</sub> (**2**), [Cd<sub>2</sub>(5-iipa)<sub>2</sub>(phen)<sub>2</sub>]<sub>n</sub> (**3**), [Mn<sub>2</sub>(5-iipa)<sub>2</sub>(phen)<sub>2</sub>]<sub>n</sub> (**4**), [Mn<sub>4</sub>(5-iipa)<sub>4</sub>(bpe)<sub>4</sub>·SH<sub>2</sub>O]<sub>n</sub> (**5**), [Co(5-iipa)(*p*-bix)]<sub>n</sub> (**6**), and [Co(5-iipa)(*m*-bix)]<sub>n</sub> (**7**).

## ■ EXPERIMENTAL SECTION

**Materials and Physical Measurements.** 5-Iodo-isophthalic acid was prepared according to the literature,<sup>25</sup> and the crystals were purified by recrystallization. All other starting materials were of analytical grade and obtained from commercial sources without further purification. Elemental analysis for C, H, and N were performed on a Perkin-Elmer 240 elemental analyzer. The FT-IR spectra were recorded from KBr pellets in the range from 4000 to 400 cm<sup>-1</sup> on a Bruker VECTOR 22 spectrometer. Thermal analyses were performed on a SDT 2960 thermal analyzer from room temperature to 800 °C at a heating rate of 20 °C/min under nitrogen flow. X-ray powder diffraction (XRD) data were collected on a Rigaku D/Max-2500PC diffractometer with Cu Kα radiation ( $\lambda = 1.5418 \text{ \AA}$ ) over the 2θ range of 5–60° with a scan speed of 5°/min at room temperature. Solid UV–visible spectra were obtained in the 200–800 nm range on a JASCO UVIDEC-660 spectrophotometer. Luminescence spectra for the solid samples were recorded on a Hitachi 850 fluorescence spectrophotometer.

**Syntheses.** The reactions of 5-iodo-isophthalic acid with divalent zinc, cadmium, manganese, and cobalt ions in the presence of ancillary nitrogen ligands (phen, bpe, *p*-bix, and *m*-bix) under hydro-(solvo)thermal conditions yielded six X-ray suitable crystals, namely, [Zn<sub>2</sub>(5-iipa)<sub>2</sub>(phen)<sub>2</sub>(H<sub>2</sub>O)]<sub>n</sub> (**1**), [Zn(5-iipa)(bpe)<sub>1.5</sub>]<sub>n</sub> (**2**), [Cd<sub>2</sub>(5-iipa)<sub>2</sub>(phen)<sub>2</sub>]<sub>n</sub> (**3**), [Mn<sub>2</sub>(5-iipa)<sub>2</sub>(phen)<sub>2</sub>]<sub>n</sub> (**4**), [Co(5-iipa)(*p*-bix)]<sub>n</sub> (**6**), and [Co(5-iipa)(*m*-bix)]<sub>n</sub> (**7**). Only precipitates are obtained in other reactions. When we attempted the method of slow evaporation of the solvent, we obtained three Mn-containing crystals in which only [Mn<sub>4</sub>(5-iipa)<sub>4</sub>(bpe)<sub>4</sub>·SH<sub>2</sub>O]<sub>n</sub> (**5**) is X-ray suitable.

[Zn<sub>2</sub>(5-iipa)<sub>2</sub>(phen)<sub>2</sub>(H<sub>2</sub>O)]<sub>n</sub> (**1**). Compound **1** was synthesized hydrothermally in a Teflon-lined stainless steel container by heating a mixture of 5-iodo-isophthalic acid (0.0146 g, 0.05 mmol), phenanthrene (0.0099 g, 0.05 mmol), Zn(NO<sub>3</sub>)<sub>2</sub>·6H<sub>2</sub>O (0.0149 g, 0.05 mmol), and KOH (0.0056 g, 0.1 mmol) in 7 mL of distilled water at 120 °C for 3 days, and then cooled to room temperature. Colorless rectangular crystals of **1** were obtained in 79% yield based on zinc. Anal. Calcd for C<sub>40</sub>H<sub>24</sub>I<sub>2</sub>N<sub>4</sub>O<sub>9</sub>Zn<sub>2</sub> (1089.17): C, 44.11; H, 2.22; N, 5.14%. Found: C, 44.06; H, 2.29; N, 5.10%. IR/cm<sup>-1</sup> (KBr): 3445(m), 3062(w), 1619(s), 1557(m), 1516(m), 1427(s), 1348(vs), 1102(m), 849(s), 776(s), 725(s).

[Zn(5-iipa)(bpe)<sub>1.5</sub>]<sub>n</sub> (**2**). A mixture of 5-iodo-isophthalic acid (0.0146 g, 0.05 mmol), 1,2-bis(4-pyridyl)ethane (bpe) (0.0091 g, 0.05

mmol), Zn(NO<sub>3</sub>)<sub>2</sub>·6H<sub>2</sub>O (0.0149 g, 0.05 mmol), and NaOH (0.0040 g, 0.1 mmol) in distilled water (7 mL) was placed in a Teflon-lined stainless steel container, heated to 160 °C for 3 days, and then cooled to room temperature. Colorless block-like crystals of **2** were obtained in 64% yield based on zinc. Anal. Calcd for C<sub>26</sub>H<sub>18</sub>IN<sub>3</sub>O<sub>4</sub>Zn (628.70): C, 49.67; H, 2.89; N, 6.68%. Found: C, 49.59; H, 2.83; N, 6.71%. IR/cm<sup>-1</sup> (KBr): 1624(s), 1603(vs), 1556(w), 1418(m), 1337(s), 1027(w), 970(w), 840(m), 775(m), 716(m), 549(m).

[Cd<sub>2</sub>(5-iipa)<sub>2</sub>(phen)<sub>2</sub>]<sub>n</sub> (**3**) and [Mn<sub>2</sub>(5-iipa)<sub>2</sub>(phen)<sub>2</sub>]<sub>n</sub> (**4**). The isomorphous complexes **3** and **4** were synthesized by a hydrothermal procedure similar to that described for **1** except using Cd(NO<sub>3</sub>)<sub>2</sub>·4H<sub>2</sub>O (0.0154 g, 0.05 mmol) or MnCl<sub>2</sub>·4H<sub>2</sub>O (0.0099 g, 0.05 mmol) instead of Zn(NO<sub>3</sub>)<sub>2</sub>·6H<sub>2</sub>O, respectively. Colorless block-like crystals of **3** were obtained in 74% yield based on cadmium. Anal. Calcd for C<sub>40</sub>H<sub>22</sub>Cd<sub>2</sub>I<sub>2</sub>N<sub>4</sub>O<sub>8</sub> (1165.22): C, 41.23; H, 1.90; N, 4.81%. Found: C, 41.19; H, 1.96; N, 4.85%. IR/cm<sup>-1</sup> (KBr): 3058(m), 1588(s), 1542(vs), 1514(m), 1425(s), 1380(s), 1363(s), 1099(m), 857(m), 776(s), 729(s). Yellow block-like crystals of **4** were obtained in 78% yield based on manganese. Anal. Calcd for C<sub>40</sub>H<sub>22</sub>I<sub>2</sub>Mn<sub>2</sub>N<sub>4</sub>O<sub>8</sub> (1050.30): C, 45.74; H, 2.11; N, 5.33%. Found: C, 45.80; H, 2.06; N, 5.26%. IR/cm<sup>-1</sup> (KBr): 3061(w), 1610(s), 1553(s), 1514(m), 1426(s), 1378(vs), 1101(m), 860(m), 775(s), 724(s).

[Mn<sub>4</sub>(5-iipa)<sub>4</sub>(bpe)<sub>4</sub>·5H<sub>2</sub>O]<sub>n</sub> (**5**). MnCl<sub>2</sub>·4H<sub>2</sub>O (0.0099 g, 0.05 mmol) in a methanol solution (2 mL) of bpe (0.0091 g, 0.05 mmol) were added to a 5 mL aqueous solution containing 5-iipa (0.0146 g, 0.05 mmol) and NaOH (0.0040 g, 0.1 mmol). The resulting reaction mixture was left unperturbed for slow evaporation of the solvent. After six days, yellow block-like crystals of **5** were obtained in 81% yield based on manganese. Anal. Calcd for C<sub>80</sub>H<sub>62</sub>I<sub>4</sub>Mn<sub>4</sub>N<sub>8</sub>O<sub>21</sub> (2198.74): C, 43.70; H, 2.84; N, 5.09%. Found: C, 43.77; H, 2.79; N, 5.02%. IR/cm<sup>-1</sup> (KBr): 3442(w), 1606(vs), 1541(m), 1425(s), 1379(vs), 1014(w), 970(w), 821(w), 778(m), 724(m), 551(s).

[Co(5-iipa)(*p*-bix)]<sub>n</sub> (**6**). Complex **6** was synthesized hydrothermally in a Teflon-lined stainless steel container by heating a mixture of 5-iodo-isophthalic acid (0.0146 g, 0.05 mmol), 1,4-bis(imidazol-1-ylmethyl)-benzene (*p*-bix) (0.0119 g, 0.05 mmol), Co(NO<sub>3</sub>)<sub>2</sub>·6H<sub>2</sub>O (0.0146 g, 0.05 mmol), and KOH (0.0056 g, 0.1 mmol) in 7 mL of distilled water at 130 °C for 4 days, and then cooled to room temperature. Purple needle crystals of **6** were obtained in 86% yield based on cobalt. Anal. Calcd for C<sub>22</sub>H<sub>17</sub>CoIN<sub>4</sub>O<sub>4</sub> (587.23): C, 44.99; H, 2.92; N, 9.54%. Found: C, 44.94; H, 2.98; N, 9.46%. IR/cm<sup>-1</sup> (KBr): 3430(w), 3093(s), 1616(vs), 1552(s), 1420(w), 1343(vs), 1249(m), 1110(m), 773(s), 724(s), 660(m).

[Co(5-iipa)(*m*-bix)]<sub>n</sub> (**7**). Complex **7** was synthesized by analogy to **6** except that 1,3-bis(imidazol-1-ylmethyl)-benzene (*m*-bix) (0.0119 g, 0.05 mmol) instead of 1,4-bis(imidazol-1-ylmethyl)-benzene (*p*-bix) and LiOH·H<sub>2</sub>O (0.0042 g, 0.1 mmol) instead of KOH. Purple needle crystals of **7** were obtained in 80% yield based on cobalt. Anal. Calcd for C<sub>22</sub>H<sub>17</sub>CoIN<sub>4</sub>O<sub>4</sub> (587.23): C, 44.99; H, 2.92; N, 9.54%. Found: C, 44.92; H, 2.87; N, 9.48%. IR/cm<sup>-1</sup> (KBr): 3122(s), 1612(vs), 1441(m), 1353(vs), 1239(m), 1104(m), 1082(s), 948(m), 862(m), 773(m), 727(s), 714(m), 655(m).

**X-ray Crystallography.** Single crystals suitable for X-ray analyses were used for intensity data collection on a Bruker SMART APEX CCD diffractometer<sup>28</sup> using graphite-monochromatized MoKα radiation ( $\lambda = 0.71073 \text{ \AA}$ ) at room temperature using the  $\omega$ -scan technique. Lorentz polarization and absorption corrections were applied. The structures were solved by direct methods with SHELXS-97<sup>29</sup> and refined with the full-matrix least-squares technique using the SHELXL-97<sup>30</sup> program. Anisotropic thermal parameters were assigned to all non-hydrogen atoms. The hydrogen atoms of the coordination water molecules and ligands were included in the structure factor calculation at idealized positions by using a riding model and refined isotropically. The hydrogen atoms of the solvent water molecules were located from the

**Table 1.** Crystal Data and Structure Refinement for 5-iipa·H<sub>2</sub>O and Compounds 1–7

compound	5-iipa·H <sub>2</sub> O	1	2	3	4	5	6	7
formula	C <sub>8</sub> H <sub>7</sub> IO <sub>5</sub>	C <sub>40</sub> H <sub>24</sub> I <sub>2</sub> <sup>-</sup> N <sub>4</sub> O <sub>9</sub> Zn <sub>2</sub>	C <sub>26</sub> H <sub>18</sub> IN <sub>3</sub> <sup>-</sup> O <sub>4</sub> Zn	C <sub>40</sub> H <sub>22</sub> Cd <sub>2</sub> I <sub>2</sub> <sup>-</sup> N <sub>4</sub> O <sub>8</sub>	C <sub>40</sub> H <sub>22</sub> I <sub>2</sub> Mn <sub>2</sub> <sup>-</sup> N <sub>4</sub> O <sub>8</sub>	C <sub>80</sub> H <sub>62</sub> I <sub>4</sub> Mn <sub>4</sub> <sup>-</sup> N <sub>8</sub> O <sub>21</sub>	C <sub>22</sub> H <sub>17</sub> <sup>-</sup> CoIN <sub>4</sub> O <sub>4</sub>	C <sub>22</sub> H <sub>17</sub> <sup>-</sup> CoIN <sub>4</sub> O <sub>4</sub>
fw	310.04	1089.17	628.70	1165.22	1050.30	2198.74	587.23	587.23
crystal system	monoclinic	monoclinic	triclinic	monoclinic	monoclinic	monoclinic	monoclinic	monoclinic
space group	P <sub>2</sub> <sub>1</sub> /c	C <sub>2</sub> /c	P <sub>1</sub>	P <sub>2</sub> <sub>1</sub> /c	P <sub>2</sub> <sub>1</sub> /c	P <sub>2</sub> /c	P <sub>2</sub> <sub>1</sub> /c	C <sub>2</sub> /c
<i>a</i> (Å)	14.341(3)	27.451(5)	9.926(2)	10.433(5)	10.247(2)	10.214(5)	10.220(1)	24.2310(3)
<i>b</i> (Å)	9.603(2)	9.517(2)	10.815(2)	14.803(7)	14.609(3)	13.885(6)	14.560(1)	10.16560(1)
<i>c</i> (Å)	7.202(1)	16.842(3)	13.742(3)	26.493(1)	26.348(7)	18.196(8)	15.010(1)	19.5257(3)
$\alpha$ (°)	90	90	106.53(3)	90	90	90	90	90
$\beta$ (°)	97.63(3)	122.08(3)	94.87(3)	109.45(2)	109.29(3)	103.17(1)	104.85(2)	114.94(2)
$\gamma$ (°)	90	90	111.80(3)	90	90	90	90	90
<i>V</i> (Å <sup>3</sup> )	983.1(3)	3728.2(2)	1282.7(6)	3858(3)	3722.8(2)	2512.7(2)	2159(3)	4361.1(3)
<i>Z</i>	4	4	2	4	4	1	4	8
<i>D<sub>c</sub></i> (g·cm <sup>-3</sup> )	2.095	1.940	1.628	2.006	1.874	1.446	1.807	1.789
$\mu$ (mm <sup>-1</sup> )	3.250	3.007	2.197	2.761	2.397	1.783	2.263	2.240
<i>F</i> (000)	592	2120	620	2224	2040	1068	1156	2312
<i>R</i> (int)	0.0502	0.0441	0.0461	0.0984	0.0308	0.0275	0.0813	0.0344
GOF	1.026	1.088	1.038	1.037	1.099	1.095	1.020	1.030
<i>R</i> <sub>1</sub> <sup>a</sup> ( <i>I</i> > 2σ( <i>I</i> ))	0.0520	0.0549	0.0515	0.0495	0.0311	0.0561	0.0545	0.0329
<i>wR</i> <sub>2</sub> <sup>b</sup> (all data)	0.1721	0.1504	0.0937	0.1259	0.0643	0.2077	0.0705	0.0787
max/min(e Å <sup>-3</sup> )	0.551/-0.628	0.794/-1.084	0.674/-0.448	1.487/-1.754	1.179/-1.020	1.175/-1.310	1.113/-1.254	0.660/-0.864

<sup>a</sup>  $R_1 = \sum |F_o| - |F_c| / \sum |F_o|$ . <sup>b</sup>  $wR_2 = \{\sum [w(F_o^2 - F_c^2)^2] / \sum [w(F_o^2)^2]\}^{1/2}$ .

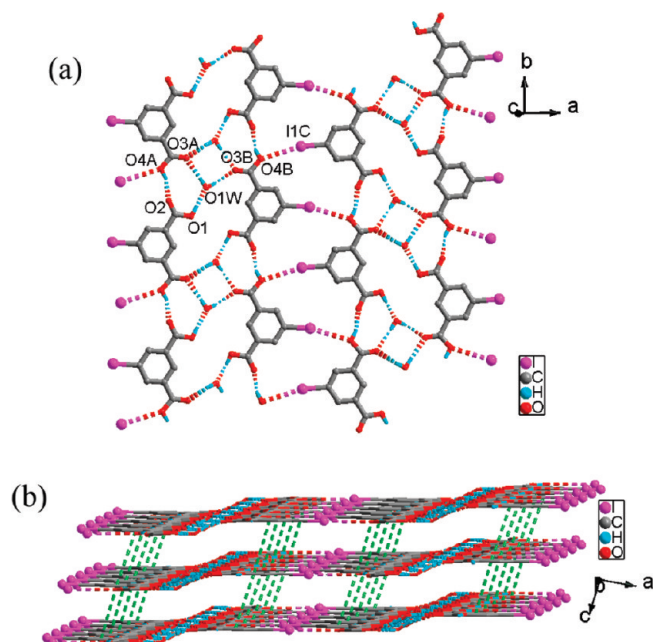


**Figure 1.** (a) A single layer in the crystal structure of 5-iipa·H<sub>2</sub>O. (Thin and thick dotted lines represent hydrogen bonds and O···I interactions, respectively. Symmetry codes: A: *x*, *y* + 1, *z*; B:  $-x + 2, -y + 1, -z$ ; C: *x* + 1,  $-y + 1.5, z - 0.5$ .) (b) 3D supramolecular structure of 5-iipa·H<sub>2</sub>O. (Green dotted lines represent the face-to-face  $\pi \cdots \pi$  interactions between adjacent layers.)

difference Fourier maps, then restrained at fixed positions and refined isotropically. Analytical expressions of neutral atom scattering factors were employed, and anomalous dispersion corrections were incorporated. In compound 5, both the site occupancies of O<sub>2</sub>W and O<sub>3</sub>W are

0.5, whereas that of O<sub>1</sub>W is 0.25. It is noteworthy that the O<sub>3</sub>W is disordered over two crystallographically split positions with the site occupancy factors of 0.21(3) and 0.29(3), respectively. The iodine atoms in 2 were disordered into two positions with site occupancy factors of 0.79(4)/0.21(4). The crystallographic data and selected bond lengths and angles for 5-iipa·H<sub>2</sub>O and 1–7 are listed in Tables 1 and S1.

## RESULTS AND DISCUSSION

**5-Iodo-isophthalic acid (5-iipa).** Crystalline 5-iodo-isophthalic acid (5-iipa) was obtained in the form of a monohydrate. Its crystal structure was determined to investigate the possible formation of halogen bonds in the process of crystallization. Along the *b*-axis, adjacent 5-iipa molecules are connected by hydrogen bonds to form an infinite chain (O<sub>4A</sub>–O<sub>2</sub>, 2.608 Å), and each pair of antiparallel neighboring chains are extended to yield a double chain by the bridging water molecule through hydrogen bonds (O<sub>1</sub>–O<sub>1</sub>W, 2.591 Å; O<sub>1</sub>W–O<sub>3A</sub>, 2.849 Å; O<sub>1</sub>W–O<sub>3B</sub>, 2.887 Å), as shown in Figure 1a. Interestingly, the distance between the nearest O atom and I atom from different chains is 3.39 Å, which is shorter than the sum of the van der Waals radii of the two atoms (ca. 3.50 Å),<sup>31</sup> indicating the existence of O···I halogen bonding. Then flat supramolecular layers are accomplished by the interconnection of double chains through O···I halogen bonds (Figure 1a). The face-to-face  $\pi \cdots \pi$  interaction between adjacent layers (intercentroid distance 3.976 Å) gives rise to the 3D supramolecular architecture (Figure 1b).

Having established the structural characteristics of 5-iipa monohydrate, we proceeded to conduct a systematic investigation of the halogen bonding effect in the assembly of metal–organic supramolecular frameworks based on 5-iipa and selected divalent metal ions. Previous structural results have proven that π-related interactions were usually found in metal–organic

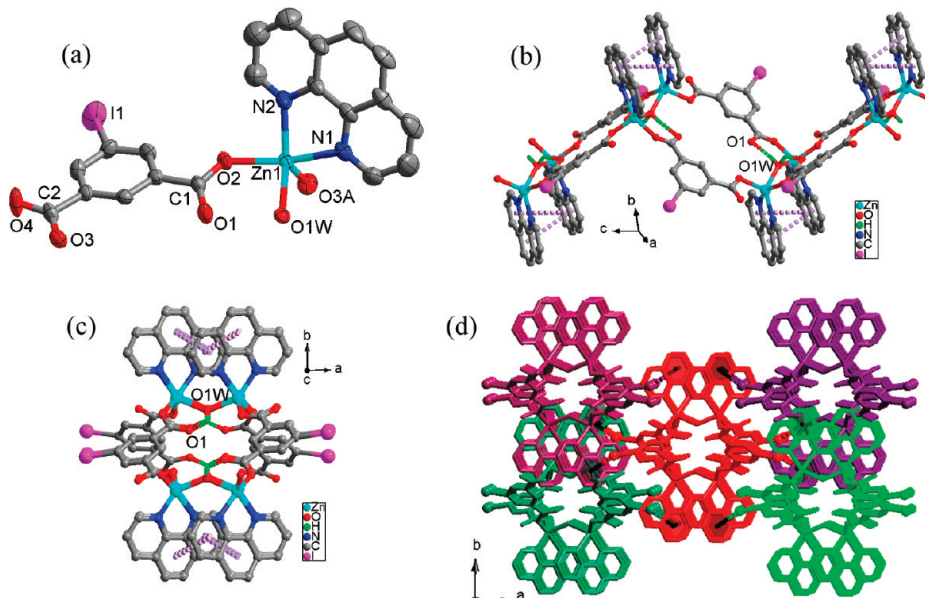


**Figure 2.** (a) Metal coordination and atom labeling in complex **1** (thermal ellipsoids at 50% probability level). All hydrogen atoms are omitted for clarity. (b) A view of the double zigzag chain in compound **1**. (Dotted lines represent hydrogen bonds and  $\pi \cdots \pi$  interactions, respectively.) (c) Top view of the double chain along the *c*-axis. (d) 3D Supramolecular structure. (Dotted lines represent  $I \cdots \pi$  interactions.)

networks with phenanthroline.<sup>32</sup> Thus, it was selected as an ancillary ligand to introduce  $I \cdots \pi$  interactions to extend the result metal–organic networks in compounds **1**, **3**, and **4**.

[Zn<sub>2</sub>(5-iipa)<sub>2</sub>(phen)<sub>2</sub>(H<sub>2</sub>O)]<sub>n</sub> (**1**). As shown in Figure 2a, in compound **1**, the Zn(II) ion is coordinated by three O atoms from two 5-iipa<sup>2-</sup> ligands, the water molecule located on a site of symmetry 2, and two N atoms from the chelating phen ligand to achieve a distorted square-pyramid geometry with a Addison trigonality factor  $\tau = 0.339$ .<sup>33</sup> Four atoms O1W, O2, N1, and N2 comprise the equatorial plane, while another atom O3A occupies the axial position. Each 5-iipa<sup>2-</sup> ligand links two Zn atoms in the μ<sub>2</sub>-bridging mode with both carboxylate groups in monodentate fashion. Two adjacent Zn atoms are bridged by the water molecule to form a bimetal unit, and neighboring units are linked through a pair of symmetry-related 5-iipa<sup>2-</sup> ligands to yield an infinite wavy ribbon (Figure 2b). Water molecule O1W is hydrogen-bonded to the adjacent O1 atom (O1W–O1, 2.568 Å) to stabilize the ribbon. The adjacent phen ligands are in parallel alignment, and  $\pi \cdots \pi$  stacking interactions occur with a face-to-face contact of 3.855 Å between two parallel aromatic rings (phenyl ring and pyridine ring bearing the N1 atom). It is noteworthy that the distance between the I atom and an adjacent phen ring of the phen ligand from another ribbon is 3.707 Å, which is indicative of weak  $I \cdots \pi$  interactions. As shown in Figure 2d, each ribbon is connected with four other ribbons through pairs of symmetry-related  $I \cdots \pi$  interactions, respectively, and then such ribbons are interconnected to yield a 3D supramolecular structure.

[Zn(5-iipa)(bpe)<sub>1.5</sub>]<sub>n</sub> (**2**). Phenanthrene ligand chelate metal cations which make it difficult to form high-dimensional structure, such as in compound **1**. To investigate the effect of coexisting ligands on the assembly of resulting metal–organic structures,<sup>34</sup> we selected the longer pillar linker bpe as the ancillary ligand and obtained complex **2**. As shown in Figure 3a, the Zn center is coordinated by three O atoms from two different 5-iipa<sup>2-</sup> ligands and three N atoms from three adjacent bpe ligands, completing a distorted octahedral coordination geometry. Each

5-iipa<sup>2-</sup> ligand acts as a μ<sub>2</sub>-bridge linking two Zn1 atoms via one chelating and one monodentate carboxylate groups to form an infinite Zn–5-iipa<sup>2-</sup> chain running along the *a*-axis. In compound **2**, there are two independent bpe ligands, one of which is located at an inversion center. One kind of bpe ligand links adjacent chains running along the *c*-axis with a dihedral angle of 68.6° for two pyridyl rings to form a (4,4)-layer with a Zn1···Zn1 distance of 9.926 and 13.742 Å, respectively (Figure 3b). These pyridyl nitrogen atoms and Zn ions are essentially in the same [1 0 1] plane. Two adjacent layers are further bridged by the other kind of μ<sub>2</sub>-bpe ligand (orange in Figure 3b) running along the direction which is almost perpendicular to the layer to result in an interesting 2D double-layered sheet with the distance between the two layers of 13.716 Å. The shortest distance of H9 to the center of the pyridine ring in the same layer is about 3.052 Å, indicating the existence of C–H···π interactions which stabilizes the double-layered structure. If 5-iipa<sup>2-</sup> and bpe ligands are considered as connectors, Zn centers can be clarified as five-connected nodes (connecting to five other Zn centers through two 5-iipa<sup>2-</sup> and three bpe ligands). Then the sheet can be simplified as a (4,5) net with a (4<sup>8</sup>·6<sup>2</sup>) Schläfli symbol. To the best of our knowledge, the (4,4) net is common in the structure of the coordination polymers based on isophthalic acid and its derivatives;<sup>35</sup> however, the 5-connected double-layered structure is relatively rare.

The channels within each double-layered sheet lead to the formation of catenation between adjacent sheets, and thus, each double sheet is bccatenated by two other sheets (one from upper and the other from lower layer) in a parallel fashion to minimize the large void cavities and stabilize the network to produce a 2D → 3D entanglement. The overall architecture is schematically represented in Figure 3c. In recent years, many particularly intriguing coordination networks have been extensively studied due to the different types of entanglements. Some examples with 2D → 3D entangled structures have been reported, in which the individual motifs with layers are catenated with some other component motifs to result in a 3D architecture.<sup>36</sup> To the best of our knowledge, most of the 2D → 3D studies have focused on

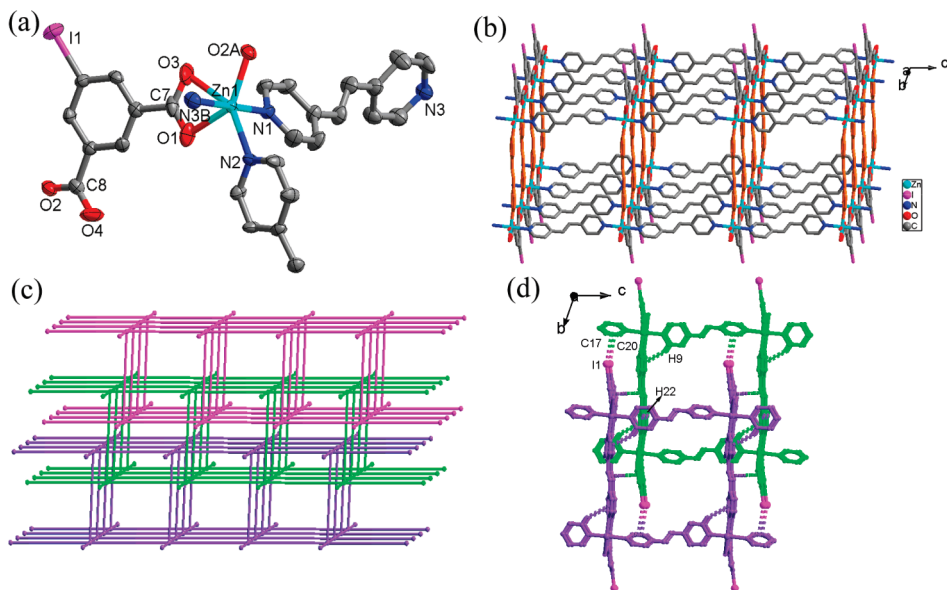


**Figure 3.** (a) Metal coordination and atom labeling in complex 2 (thermal ellipsoids at 50% probability level). All hydrogen atoms are omitted for clarity. (b) The double layer in compound 2. One kind of connecting bpe ligand is marked in orange. (c) The schematic view of the 2D  $\rightarrow$  3D interpenetration. (d) The supramolecular interactions between interpenetrated layers.

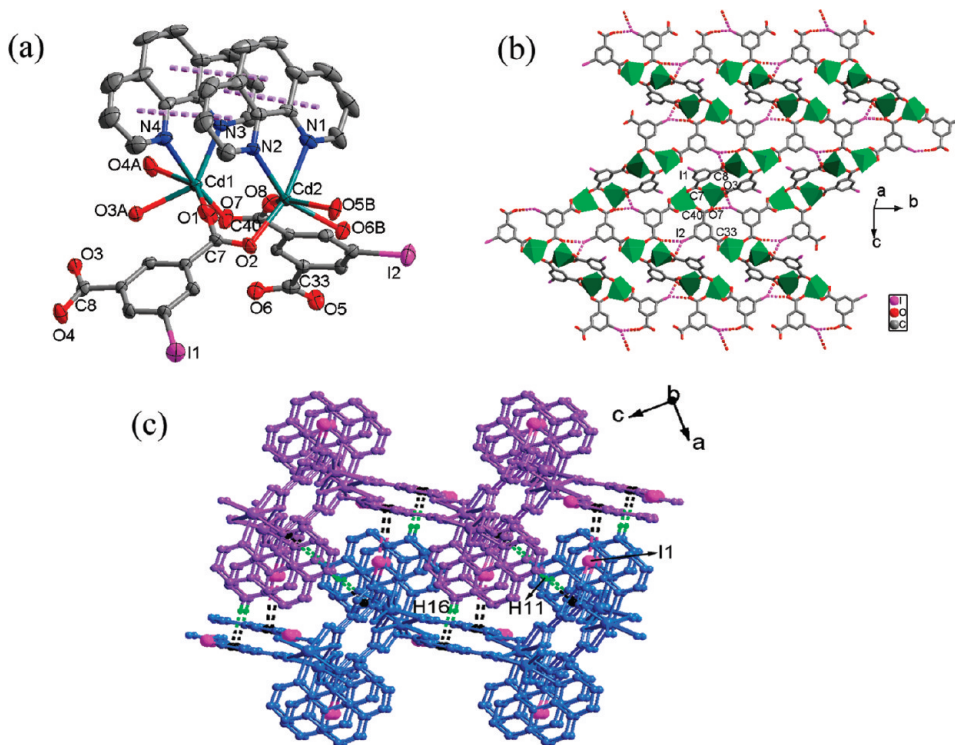


**Figure 4.** (a) Metal coordination and atom labeling in complex 3 (thermal ellipsoids at 50% probability level). All hydrogen atoms are omitted for clarity. (Dotted lines represent  $\pi \cdots \pi$  interactions.) (b) The 2D structure of compound 3. Phen ligands are omitted for clarity. Cd atoms are drawn as polyhedrons (Cd1: sea green, Cd2: bright green). (Dotted lines represent I  $\cdots$  O interactions.) (c) 3D supramolecular structure of 3 (pink: I, green: H, black: the center of the phenyl ring).

the parallel<sup>37</sup> or inclined<sup>38</sup> catenation of monolayers, while catenated bilayers are relatively less common.<sup>39</sup>

The open space within each bilayer leads to the formation of catenation between adjacent bilayers that are parallel to one another and crystallographically equivalent. It is worth noting

that many different weak supramolecular interactions coexist in adjacent pieces, which are responsible for stabilizing the overall 3D architecture. The distance between the I atom and proximal edge (C17–C20) from different pieces are 3.461 Å, indicating the existence of weak I  $\cdots$   $\pi$  interactions. The interpenetrating

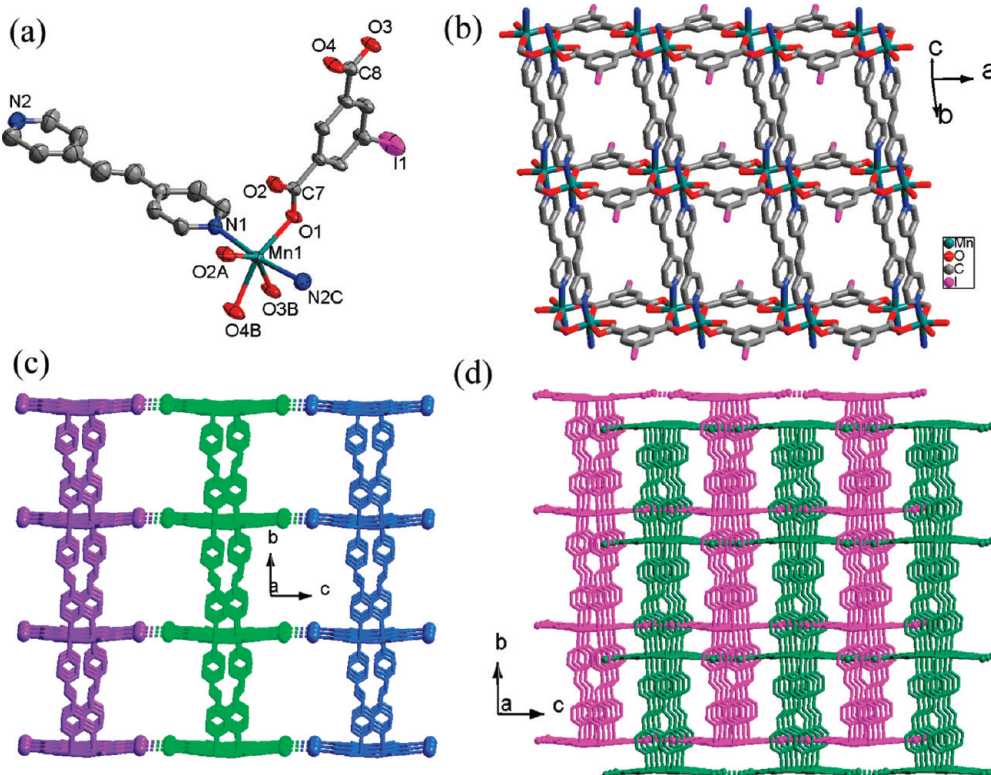


**Figure 5.** (a) Metal coordination and atom labeling in complex 5 (thermal ellipsoids at 50% probability level). All hydrogen atoms and water molecules are omitted for clarity. (b) The pillared layer structure of 5. (c) 3D supramolecular structure of 5. (Dotted lines represent I...I interactions.) (d) A view of the interpenetrating 3D framework.

pieces are also stabilized by  $\pi\cdots\pi$  [center (ethylene group)—center (C1—C6): 3.447 Å] and C—H $\cdots\pi$  [H9—center (N2, C21—C25): 3.05 Å; H22—center (N1, C9—C13): 3.08 Å] interactions, as shown in Figure 3d.

**[Cd<sub>2</sub>(5-iipa)<sub>2</sub>(phen)<sub>2</sub>]<sub>n</sub>** (3). When Cd and Mn were used instead of Zn, structurally different frameworks were found in compounds 3 and 4 under similar reaction conditions. The asymmetric unit of 3 consists of two crystallographically independent Cd(II) atoms, two 5-iipa<sup>2-</sup> ligands, and two phen ligands. Two phen ligands are arranged in parallel mode and stabilized by face-to-face  $\pi\cdots\pi$  interactions [intercentered distance: 3.954 Å (N1-ring—N3-ring), 4.036 Å (phenyl rings), 3.976 Å (N2-ring—N4-ring)] (Figure 4a). Each Cd ion is in a distorted octahedral coordination environment and coordinated by four oxygen atoms from two 5-iipa<sup>2-</sup> ligands and two nitrogen atoms from the chelating phen molecule. Cd1 and Cd2 are first bridged by two carboxylate groups (C7, C40) which come from two different 5-iipa<sup>2-</sup> ligands to form a Cd<sub>2</sub>(CO<sub>2</sub>)<sub>2</sub> binuclear cluster, and two symmetry related clusters are further linked by a pair of symmetry related 5-iipa<sup>2-</sup> ligands (C7, C8) with one carboxylate (C7) in bridging and the other one (C8) in chelating mode to result in a tetranuclear unit. Such units are further connected together through another 5-iipa<sup>2-</sup> (C33, C40) to generate a layer structure. It is interesting to notice that the distances of O—I are 3.449 Å (O3—I2) and 3.349 Å (O7—I2), respectively, which indicate that there are O $\cdots$ I halogen bonds within the layer (Figure 4b). Adjacent layers are first associated together through I $\cdots\pi$  interactions (I—centroid distance, 3.925 Å) between the iodine atoms and the neighboring aromatic rings from 5-iipa<sup>2-</sup> ligands in the adjacent layers to lead to a 3D

supramolecular structure. The aromatic rings from phen and adjacent phenyl rings of 5-iipa<sup>2-</sup> ligands which come from different layers are arranged almost mutually perpendicular, which is ideally situated for the formation of the C—H $\cdots\pi$  interactions (H11—centroid: 2.789 Å, H16—centroid: 2.632 Å). Then, adjacent layers are further organized together through such C—H $\cdots\pi$  interactions to stabilize the 3D supramolecular architecture (Figure 4c).

**[Mn<sub>2</sub>(5-iipa)<sub>2</sub>(phen)<sub>2</sub>]<sub>n</sub>** (4). Compound 4 is isostructural with 3. The distances between the adjacent O atom and I atom are 3.361 Å (O1—I2), 3.442 Å (O3—I2), respectively.

**[Mn<sub>4</sub>(5-iipa)<sub>4</sub>(bpe)<sub>4</sub>·5H<sub>2</sub>O]<sub>n</sub>** (5). The asymmetric unit of compound 5 contains one 5-iipa<sup>2-</sup> ligand, one Mn(II) ion, one bpe ligand as well as one and a quarter water molecules. The coordination environment of Mn1 is represented in Figure 5a, the Mn(II) atom is bonded to four carboxylate oxygen atoms from three different 5-iipa<sup>2-</sup> ligands and two pyridyl nitrogen atoms from two different bpe ligands to form a distorted octahedral geometry. Pairs of symmetry-related 5-iipa<sup>2-</sup> ligands act as bridges joining adjacent Mn(II) bimetal pairs to result in a [Mn<sub>2</sub>(5-iipa)<sub>2</sub>]<sub>n</sub> double chain, and such chains are further linked by bpe ligands running along the *b*-axis to furnish a 2D pillared layer in the *ab* plane, as illustrated in Figure 5b. More interestingly, the distance between the adjacent iodine atoms of 3.627 Å are considerably shorter than the sum of the van der Waals radii of the two atoms (ca. 4.0 Å) which indicate there are I $\cdots$ I interactions between the iodine atoms. When the I $\cdots$ I halogen bonding between layers are taken into account, the resulting net of 5 becomes a 3D architecture with large channels (ca. 13.885  $\times$  17.750 Å<sup>2</sup>). It is a rare example in the metal—organic networks.

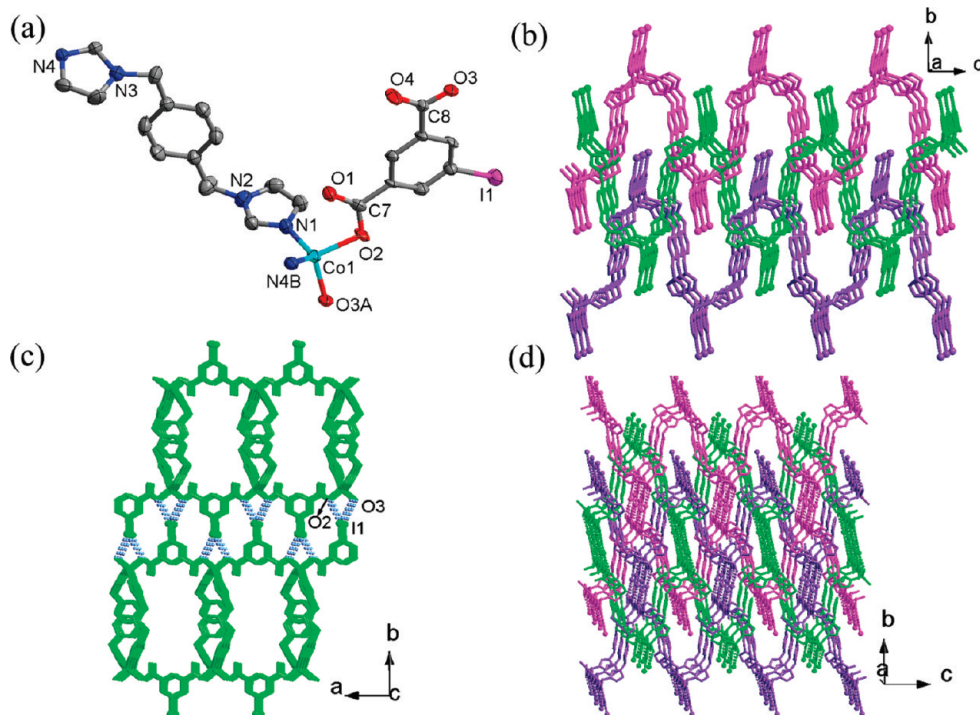


**Figure 6.** (a) Metal coordination and atom labeling in complex 6 (thermal ellipsoids at 50% probability level). All hydrogen atoms are omitted for clarity. (b) The 2D → 3D interpenetrating structure in 6. (c) 3D supramolecular structure sustained by O···I interactions in 6. (Dotted lines represent O···I interactions.) (d) A view of the 3-fold 3D interpenetration for 6.

A further investigation reveals a more striking feature of **5**; that is, two sets of the 3D architectures are interlaced in a parallel fashion to give rise to a 2-fold interpenetrating structure (Figure 5d) to minimize the open channels and stabilize the architecture. In recent years, interpenetrating nets in which independent motifs are entangled together in different ways have been widely reported for coordination polymers through covalent bonds or other noncovalent interactions in the literature.<sup>15a,40</sup> The interpenetrating structures supported by halogen bonding and related I···I and I···π intermolecular interactions are still rare. As far as we know, only very limited examples with interpenetrating systems based on halogen bonds have been reported,<sup>41</sup> while 3D networks formed by metal–organic layers via I···I interactions interdigitating with each other have not been found up to now.

[Co(5-iipa)(*p*-bix)]<sub>n</sub> (**6**). As shown in Figure 6a, the asymmetric unit of **6** contains one Co(II) ion, one 5-iipa<sup>2-</sup> ligand, and one *p*-bix ligand. Each Co(II) atom is four coordinated by two O atoms from two 5-iipa<sup>2-</sup> ligands, and two N atoms from two *p*-bix ligands to complete a distorted tetrahedral environment. The 5-iipa<sup>2-</sup> ligand adopts a μ<sub>2</sub>-bridge coordination mode through bimonodentate carboxylate moieties linking two Co centers to form an infinite chain along the *a*-axis, which are expanded into a 2D under layer through μ<sub>2</sub>-bridged *p*-bix ligands. It is interesting to notice that each under layer is entangled by two other layers to achieve a 2D → 3D interpenetrating structure (Figure 6b). More interesting, the short distances between I atom and the nearest O atoms which come from two adjacent layers (O2···I, 3.312 Å and O3···I, 3.453 Å) indicate interlayer O···I halogen bonding (Figure 6c), which connect the adjacent layers to form a 3D supramolecular structure, and three sets of such supramolecular structures are interlocked with each other to display a 3-fold interpenetrating architecture, as shown in Figure 6d. To the best

of our knowledge, it is the first example of a 3-fold interpenetrating supramolecular structure in which metal–organic sheets are linked together through halogen bonding.

In the same covalent layer, the Co center is linked by four different Co atoms through two 5-iipa<sup>2-</sup> and two bix molecules. Taking account of the O···I halogen bonding, the Co center is also connected by two other Co atoms through O···I halogen bonding together with one 5-iipa<sup>2-</sup> from an adjacent metal–organic layer. If the metal centers and the ligands can be seen as nodes and rods, respectively, the whole architecture of **6** can be simplified as a 3-fold interpenetrating structure by a 6-connected network with a Schläfli symbol of (3<sup>3</sup>4<sup>6</sup>5<sup>5</sup>6) topology (Figure S1, Supporting Information).

[Co(5-iipa)(*m*-bix)]<sub>n</sub> (**7**). Compound **7** contains an unusual 2-fold interpenetration architecture connected by O···I halogen bonding. As illustrated in Figure 7a, each Co(II) ion is five-coordinated and adopts a distorted trigonal bi pyramid environment formed by one chelating carboxylate group from a 5-iipa<sup>2-</sup> ligand, one carboxylate oxygen from another 5-iipa<sup>2-</sup> ligand, and two nitrogen atoms from two different *m*-bix molecules. Adjacent Co(II) ions are associated together by the 5-iipa<sup>2-</sup> ligand with one carboxylate in monodentating fashion and the other one in bidentate chelating fashion to form a chain running along the *b*-axis. Interestingly, neighboring chains are antiparallel to each other. The N-containing ligand bridges the chains in TG conformation to form a (4,4) net with Co···Co distances of 10.166 and 12.299 Å (Figure 7b). It should be noted that adjacent layers are associated by interlayer O···I interactions (Figure 7c) with the distance between O3 and I1 atom of 3.474 Å to form a 3D supramolecular structure. Two sets of such supramolecular structures are interlocked with each other in an antiparallel fashion to display a centrosymmetric 2-fold interpenetrating architecture,

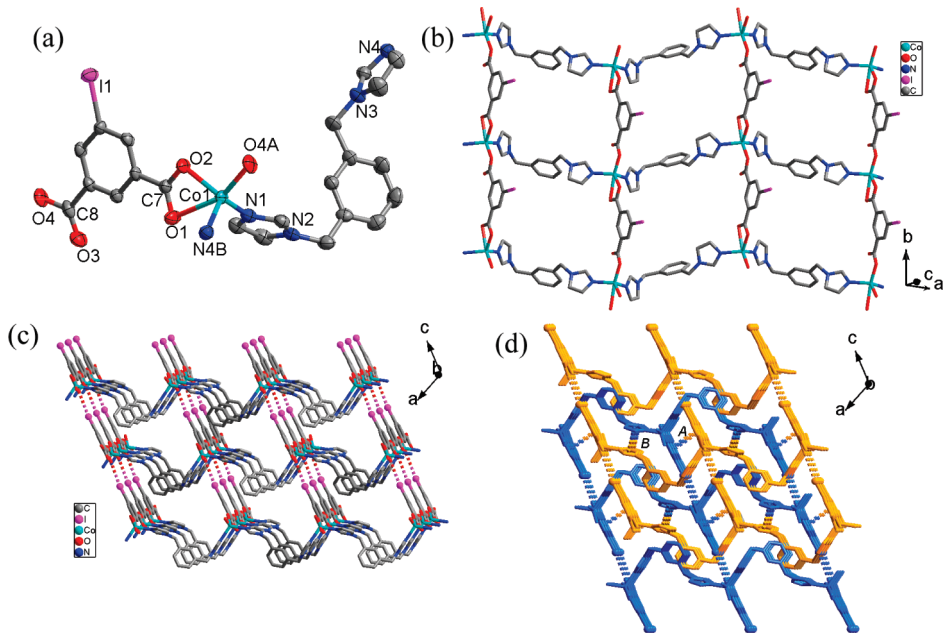


**Figure 7.** (a) Metal coordination and atom labeling in complex 7 (thermal ellipsoids at 50% probability level). All hydrogen atoms are omitted for clarity. (b) The 2D layer. (c) The 3D net connected by interlayer O...I halogen bonding. (Dotted lines represent O...I halogen bonding.) (d) The 2-fold interpenetration. Two colored dotted lines represent  $\pi\cdots\pi$  interactions. A and B represent the  $\pi\cdots\pi$  interactions between two benzene rings and two imidazole rings, respectively.

as shown in Figure 7d. Meanwhile, the whole structure is reinforced by aromatic  $\pi\cdots\pi$  interactions with the centroid-to-centroid distance between the benzene rings of 5-iipa<sup>2-</sup> and imidazole rings of *m*-bix ligands from different motifs being 3.749 and 3.853 Å, respectively.

## ■ DISCUSSION

**The Effect of Halogen-Related Interactions in the Assembly of Coordination Polymers.** As we all know, isophthalic acid and its derivatives with different functional substituted -R groups (-OH, -COOH, -NO<sub>2</sub>, -NH<sub>2</sub>, -Me, -MeO, or -C(CH<sub>3</sub>)<sub>3</sub>, etc.) at the 5-position are good dicarboxylate-bridging ligands to construct coordination polymers in which many supramolecular structures have been furnished.<sup>35</sup> Compared with these ligands, the introduction of the polarizable iodine atom makes it possible to generate distinct complexes. Most of the corresponding complexes with isophthalic acid or other derivates and the same metal ion/coligand are different from our structures, such as [Cd(mpa)(phen)]<sub>n</sub><sup>35a</sup> [{Zn<sub>3</sub>(μ<sub>3</sub>-OH)(ophen)<sub>3</sub>} (ipa)<sub>2</sub>{Zn<sub>3</sub>(μ<sub>3</sub>-OH)(ophen)<sub>3</sub>}]<sub>n</sub>·0.5H<sub>2</sub>O,<sup>42a</sup> {[Zn(dpe)(OH-BDC)](dpe)<sub>0.5</sub>}<sub>n</sub><sup>42b</sup> {[Mn(tbip)(dpe)]·1.5H<sub>2</sub>O}<sub>n</sub><sup>35f</sup> and so on. The layer structure of the [Mn(ip)(dpe)]<sub>n</sub>·0.5ndpe·nH<sub>2</sub>O<sup>43</sup> is similar to that in [Mn<sub>4</sub>(5-iipa)<sub>4</sub>(bpe)<sub>4</sub>·5H<sub>2</sub>O]<sub>n</sub> (5); however, the layer structure in 5 is expanded to a 3D supramolecular architecture through I...I interactions and form a 2-fold interpenetration. The difference may be ascribed to the effect of the polarizable iodine atom in 5-iipa, which provides a new approach to use halogen-related interactions in combination with metal coordination in the assembly of the supramolecular structures. As shown in Table 2, various intermolecular halogen-related interactions have been found in the titled structures. According to previous research, many intermolecular interactions such as hydrogen bonding and  $\pi\cdots\pi$  interactions contribute to the stabilities of the structure.<sup>18,19</sup> The existence of the

**Table 2. The Related Information of Halogen Bonding in Compounds 1–7**

compound	halogen bonding (D...I-C)	<i>d</i> (D...I) (Å)	$\angle$ DIC (deg)	influence
1	$\pi\cdots\text{I-C}$	3.707	143.0	1D → 3D
2	$\pi\cdots\text{I-C}$	3.461	163.4	to reinforce the structure
3	O...I-C	3.349	147.6	to reinforce the structure
		3.449	139.5	
	$\pi\cdots\text{I-C}$	3.928	139.9	2D → 3D
4	O...I-C	3.361	142.4	to reinforce the structure
		3.442	146.1	
	$\pi\cdots\text{I-C}$	3.913	139.4	2D → 3D
5	I...I-C	3.627	174.4	2D → 3D
6	O...I-C	3.312	153.7	2D → 3D
		3.453	152.5	
7	O...I-C	3.473	171.6	2D → 3D

halogen bonding between different motifs indicates that such intermolecular interactions play important roles in the stabilities of the whole crystal structure. In compound 2,  $\pi\cdots\text{I-C}$  interactions existing in adjacent pieces may contribute to the stability of the whole structure. The  $\pi\cdots\text{I-C}$ , O...I-C, and I...I-C interactions in other compounds help to increase the dimensionality of the structures and result in intriguing architectures respectively. In addition, taking account of the halogen bonding, the changes of the 2D → 3D in compounds 5, 6, and 7 make them turn into rare 2- or 3-fold interpenetrating supramolecular arrays based on such interactions.

**The Effect of Auxiliary Ligands.** The use of these auxiliary ligands has a significant influence on the structure. Chelating phen ligands make it possible to retain a low-dimensional structure and provide potential supramolecular recognition sites for  $\pi$ -related

interactions, such as in **1**, **3**, and **4**, whereas in **2**, **5**, **6**, and **7**, bpe, *p*-bix, and *m*-bix ligands, with certain spacers between the two pyridyl or imidazole rings, behave as a good space extender and make it easy to form a higher-dimensional architecture.

**Thermogravimetric Analysis and X-ray Powder Diffraction.** Thermogravimetric analysis (TG) of complexes **1–7** was performed to study the thermal stability of these polymers. TG curves for complexes **1–7** are shown in Figure S2, Supporting Information. For complex **1**, a gradual weight loss between 35 and 172 °C is attributed to the release of the coordinated water molecules (observed, 1.66%; calculated, 1.65%). The decomposition of the anhydrous composition is observed from 222 to 619 °C. For compound **2**, a gradual weight loss from 210 °C indicates the removal of the organic components. In the case of compound **3**, no obvious weight loss was observed until the temperature rose to 363 °C. For compound **4**, the framework collapsed from 405 °C. The TG curve of **5** shows that this complex loses its uncoordination water molecules between 45 to 128 °C (observed, 3.89%; calculated, 4.09%). The rapid weight loss was observed from 292 °C, which indicated the decomposition of the whole structure. The TG analysis for crystal samples of **6** shows the framework collapsed in the temperature range of 370–450 °C. In the case of **7**, the host framework starts to decompose beyond 393 °C, indicating the high thermal stability of this compound. According to the above thermogravimetric analysis of the seven coordination polymers, the anhydrous composition of these compounds begins to decompose beyond 210 °C; especially the frameworks of **3**, **4**, **6**, and **7** collapsed from 363, 405, 370, and 393 °C, respectively, which indicated the high thermal stability of these metal–organic materials.

X-ray powder diffraction (XRD) was used to check the purity of compounds **1–7**. As shown in Figure S3, Supporting Information, all the peaks displayed in the measured patterns (b) are similar to those in the simulated patterns generated from single-crystal diffraction data (a), indicating single phases of **1–7** are formed.

**UV/vis Absorbance Properties and Photoluminescent Properties.** The solid-state UV/vis spectra of 5-iipa and coordination polymers **1–7** are displayed in Figure S4, Supporting Information. The 5-iipa ligand itself displays weak absorption bands at 317 nm with a weak shoulder band at 379 nm, arising from the  $\pi-\pi^*$  transition of the aromatic rings.<sup>44</sup> These bands are not strongly perturbed upon its coordination to zinc(II), cadmium(II), manganese(II), and cobalt(II), suggesting that coordination of the metal ions hardly alters the intrinsic electronic properties of the ligand. For compounds **4** and **5**, the additional bands at ca. 396 nm probably originate from d-d spin-forbidden transition of the  $d^5$  ( $Mn^{2+}$ ) ion. The absorptions of **6** and **7** in the visible region are observed at ca. 547 nm, which may result from the d-d spin-allowed transition of the  $d^7$  ( $Co^{2+}$ ) ion. The difference in the UV/vis absorption properties may trace back to a discrepancy in the central metal atoms of the crystals.

As the inorganic–organic hybrid coordination polymers with  $d^{10}$  metal centers,<sup>45</sup> the emission spectra of complexes **1–3** in the solid state are investigated at room temperature. As shown in Figure S5, Supporting Information, excitation at 290 nm leads to weak violet fluorescent emission bands at 394 nm for **1** which can probably be assigned to the intraligand ( $\pi-\pi^*$ ) fluorescent emission because similar emissions are observed for the free 5-iipa at 395 nm, whereas for compounds **2** and **3** no clear luminescence was detected under the experimental conditions.

## CONCLUSION

In this study, we have synthesized and characterized seven novel coordination polymers based on 5-iodo-isophthalic acid and ancillary nitrogen ligands. As expected, structural determinations of these compounds have demonstrated that 5-iipa can act as an effective bridging ligand and its tethered iodine atom plays an important role in the assembly of the coordination polymers with increasing in dimensionality as well as the stability of the *n*-fold interpenetrated structure in compounds **1–7**. Furthermore, the interplay of coordination, halogen bonding, hydrogen bonds,  $\pi \cdots \pi$  and C–H  $\cdots \pi$  interactions in these complexes also highlights the complexity and challenge in programming the supramolecular assembly of metal–organic networks. Additional research will focus on the detailed influences of halogen bonding on the coordination assembly.

## ASSOCIATED CONTENT

**S Supporting Information.** X-ray crystallographic files (CIF), TG curves, XRD patterns, UV–vis absorption, and photoluminescent spectra. This material is available free of charge via the Internet at <http://pubs.acs.org>.

## AUTHOR INFORMATION

### Corresponding Author

\*E-mail: zangsqzg@zzu.edu.cn. Fax: (+86)-371-6778 0136.

## ACKNOWLEDGMENT

We gratefully acknowledge financial support by the National Natural Science Foundation of China (No. 20901070) and Zhengzhou University (P. R. China).

## REFERENCES

- (a) Metrangolo, P.; Resnati, G. Halogen Bonding. In *Encyclopedia of Supramolecular Chemistry*; Marcel Dekker: New York, 2004, 628–635; (b) Metrangolo, P.; Neukirch, H.; Pilati, T.; Resnati, G. *Acc. Chem. Res.* **2005**, *38*, 386–395. (c) Metrangolo, P.; Resnati, G.; Pilati, T.; Biella, S. Halogen Bonding: Fundamentals and Applications. In *Structural Bonding (Berlin)*; Springer: Berlin, 2008; Vol. 126, pp 105–136.
- (2) (a) Jagarlapudi, A. R.; Sarma, P.; Desiraju, G. R. *Acc. Chem. Res.* **1986**, *19*, 222–228. (b) Desiraju, G. R.; Parthasarathy, R. *J. Am. Chem. Soc.* **1989**, *111*, 8725–8726. (c) Reddy, C. M.; Kirchner, M. T.; Gundakaram, R. V.; Padmanabhan, K. A.; Desiraju, G. R. *Chem.—Eur. J.* **2006**, *12*, 2222–2234. (d) Awwadi, F. F.; Willett, R. D.; Peterson, K. A.; Twamley, B. *J. Phys. Chem. A* **2007**, *111*, 2319–2328. (e) Schollmeyer, D.; Shishkin, O. V.; Rühl, T.; Vysotsky, M. O. *CrystEngComm* **2008**, *10*, 715–723.
- (3) (a) Casnati, A.; Liantonio, R.; Metrangolo, P.; Resnati, G.; Ungaro, R.; Ugozzoli, F. *Angew. Chem., Int. Ed.* **2006**, *45*, 1915–1918. (b) Metrangolo, P.; Meyer, F.; Pilati, T.; Resnati, G.; Terraneo, G. *Angew. Chem., Int. Ed.* **2008**, *47*, 6114–6127. (c) Metrangolo, P.; Carcenac, Y.; Lahtinen, M.; Pilati, T.; Rissanen, K.; Vij, A.; Resnati, G. *Science* **2009**, *323*, 1461–1464. (d) Casnati, A.; Cavallo, G.; Metrangolo, P.; Resnati, G.; Ugozzoli, F.; Ungaro, R. *Chem.—Eur. J.* **2009**, *15*, 7903–7912. (e) Abate, A.; Brischetto, M.; Cavallo, G.; Lahtinen, M.; Metrangolo, P.; Pilati, T.; Radice, S.; Resnati, G.; Rissanen, K.; Terraneo, G. *Chem. Commun.* **2010**, *46*, 2724–2726.
- (4) (a) Thallapally, P. K.; Desiraju, G. R.; Bagieu-Beucher, M.; Masse, R.; Bourgogne, C.; Nicoud, J.-F. *Chem. Commun.* **2002**, 1052–1053. (b) George, S.; Nangia, A.; Lam, C.-K.; Mak, T. C. W.; Nicoud, J.-F. *Chem. Commun.* **2004**, 1202–1203. (c) Saha, B. K.; Nangia, A.;

- Jaskolski, M. *CrystEngComm* **2005**, *7*, 355–358. (d) Sun, A.; Lauher, J. W.; Goroff, N. S. *Science* **2006**, *312*, 1030–1033. (e) Espallargas, G. M.; Brammer, L.; Sherwood, P. *Angew. Chem., Int. Ed.* **2006**, *45*, 435–440. (f) Saha, B. K.; Nangia, A.; Nicoud, J.-F. *Cryst. Growth Des.* **2006**, *6*, 1278–1281. (g) Muniappan, S.; Lipstman, S.; Goldberg, I. *Chem. Commun.* **2008**, 1777–1779. (h) Cinčić, D.; Friščić, T.; Jones, W. *Chem.—Eur. J.* **2008**, *14*, 747–753. (i) Arman, H. D.; Giesecking, R. L.; Hanks, T. W.; Pennington, W. T. *Chem. Commun.* **2010**, *46*, 1854–1856.
- (S) (a) Auffinger, P.; Hays, F. A.; Westhof, E.; Ho, P. S. *Proc. Natl. Acad. Sci. U.S.A.* **2004**, *101*, 16789–16794. (b) Voth, A. R.; Khuu, P.; Oishi, K.; Ho, P. S. *Nat. Chem.* **2009**, *1*, 74–79.
- (6) Sarwar, M. G.; Dragisic, B.; Sagoo, S.; Taylor, M. S. *Angew. Chem., Int. Ed.* **2010**, *49*, 1674–1677.
- (7) Fourmigüé, M.; Batail, P. *Chem. Rev.* **2004**, *104*, 5379–5418.
- (8) (a) Loc Nguyen, H.; Horton, P. N.; Hursthouse, M. B.; Legon, A. C.; Bruce, D. W. *J. Am. Chem. Soc.* **2004**, *126*, 16–17. (b) Metrangolo, P.; Präsang, C.; Resnati, G.; Liantonio, R.; Whitwood, A. C.; Bruce, D. W. *Chem. Commun.* **2006**, 3290–3292. (c) Präsang, C.; Loc Nguyen, H.; Horton, P. N.; Whitwood, A. C.; Bruce, D. W. *Chem. Commun.* **2008**, 6164–6166.
- (9) Reddy, C. M.; Kirchner, M. T.; Gundakaram, R. C.; Padmanabhan, K. A.; Desiraju, G. R. *Chem.—Eur. J.* **2006**, *12*, 2222–2234.
- (10) (a) Sarma, J. A. R. P.; Allen, F. H.; Hoy, V. J.; Howard, J. A. K.; Thaimattam, R.; Biradha, K.; Desiraju, G. R. *Chem. Commun.* **1997**, 101–102. (b) Saha, B. K.; Nangia, A.; Nicoud, J.-F. *Cryst. Growth Des.* **2006**, *6*, 1278–1281. (c) Cariati, E.; Forni, A.; Biella, S.; Metrangolo, P.; Meyer, F.; Resnati, G.; Righetto, S.; Tordini, E.; Ugo, R. *Chem. Commun.* **2007**, 2590–2592.
- (11) Laguna, A.; Lasanta, T.; López-de-Luzuriaga, J. M.; Monge, M.; Naumov, P.; Olmos, M. E. *J. Am. Chem. Soc.* **2010**, *132*, 456–457.
- (12) (a) Shirman, T.; Freeman, D.; Posner, Y. D.; Feldman, I.; Facchetti, A.; van der Boom, M. E. *J. Am. Chem. Soc.* **2008**, *130*, 8162–8163. (b) Shirman, T.; Arad, T.; van der Boom, M. E. *Angew. Chem., Int. Ed.* **2010**, *49*, 926–929.
- (13) (a) Corradi, E.; Meille, S. V.; Messina, M. T.; Metrangolo, P.; Resnati, G. *Angew. Chem., Int. Ed.* **2000**, *39*, 1782–1786. (b) Åkeröy, C. B.; Fasulo, M.; Schultheiss, N.; Desper, J.; Moore, C. *J. Am. Chem. Soc.* **2007**, *129*, 13772–13773. (c) Metrangolo, P.; Resnati, G. *Science* **2008**, *321*, 918–919. (d) Legon, A. C. The Interaction of Dihalogens and Hydrogen Halides with Lewis Bases in the Gas Phase: An Experimental Comparison of the Halogen Bond and the Hydrogen Bond. In *Struct. Bonding (Berlin)*; Springer: Berlin/Heidelberg, 2008; Vol. 126, pp 17–64; (e) Awwadi, F. F.; Willett, R. D.; Twamley, B. *J. Mol. Struct.* **2009**, *918*, 116–122.
- (14) (a) *Crystal Design: Structure and Function*; Desiraju, G. R., Eds.; Wiley: New York, 2003; (b) *Frontiers in Crystal Engineering*; Tiekkink, E. R. T., Vittal, J. J., Eds.; Wiley: New York, 2006; Vol. 1; (c) Desiraju, G. R. *Angew. Chem. Int. Ed.* **2007**, *46*, 8342–8356.
- (15) (a) Batten, S. R.; Robson, R. *Angew. Chem., Int. Ed.* **1998**, *37*, 1460–1494. (b) Robson, R. *J. Chem. Soc., Dalton Trans.* **2000**, 3735–3744. (c) Carlucci, L.; Ciani, G.; Proserpio, D. M. *Coord. Chem. Rev.* **2003**, *246*, 247–289. (d) Åkeröy, C. B.; Champness, N. R.; Janiak, C. *CrystEngComm* **2010**, *12*, 22–43.
- (16) Special issue for metal–organic frameworks. *Chem. Soc. Rev.* **2009**, *38*, 1409–1860.
- (17) (a) Sarma, J. A. R. P.; Desiraju, G. R. *Acc. Chem. Res.* **1986**, *19*, 222–228. (b) Desiraju, G. R. *Angew. Chem., Int. Ed.* **1995**, *34*, 2311–2327. (c) Jeffrey, G. A. *An Introduction to Hydrogen Bonding*; Oxford University Press: Oxford, 1997; (d) Desiraju, G. R. Hydrogen Bonding. In *Encyclopedia of Supramolecular Chemistry*; Atwood, J. L.; Steed, J. W., Eds.; Marcel Dekker Inc.: New York, 2004; pp 658–665.
- (18) (a) Goldberg, I. *Chem.—Eur. J.* **2000**, *6*, 3863–3870. (b) Baudron, S. A.; Avarvari, N.; Batail, P. *Inorg. Chem.* **2005**, *44*, 3380–3382. (c) Heinze, K.; Reinhart, A. *Inorg. Chem.* **2006**, *45*, 2695–2703. (d) Telfer, S. G.; Wuest, J. D. *Cryst. Growth Des.* **2009**, *9*, 1923–1931. (e) Baudron, S. A.; Salazar-Mendoza, D.; Hosseini, M. W. *CrystEngComm* **2009**, *11*, 1245–1254.
- (19) (a) Zhao, L.; Chen, X.-D.; Mak, T. C. W. *Organometallics* **2008**, *27*, 2483–2489. (b) Khavasi, H. R.; Fard, M. A. *Cryst. Growth Des.* **2010**, *10*, 1892–1896. (c) Zheng, Y.-Z.; Speldrich, M.; Kögerler, P.; Chen, X.-M. *CrystEngComm* **2010**, *12*, 1057–1059.
- (20) (a) Nishio, M.; Hirota, M.; Umezawa, Y. *The CH/π Interaction: Evidence, Nature and Consequences*; Wiley-VCH, Weinheim, 1998; (b) Nishio, M. *CrystEngComm* **2004**, *6*, 130–158.
- (21) Bertani, R.; Sgarbossa, P.; Venzo, A.; Lelj, F.; Amati, M.; Resnati, G.; Pilati, T.; Metrangolo, P.; Terraneo, G. *Coord. Chem. Rev.* **2010**, *254*, 677–695.
- (22) Åkeröy, C. B.; Schultheiss, N.; Desper, J.; Moore, C. *CrystEngComm* **2007**, *9*, 421–426.
- (23) (a) Lapadula, G.; Judaš, N.; Friščić, T.; Jones, W. *Chem.—Eur. J.* **2010**, *16*, 7400–7403. (b) Smart, P.; Minguez Espallargas, G.; Brammer, L. *CrystEngComm* **2008**, *10*, 1335–1344.
- (24) Brammer, L.; Minguez Espallargas, G.; Libri, S. *CrystEngComm* **2008**, *10*, 1712–1727.
- (25) Park, J. S.; Wilson, J. N.; Hardcastle, K. I.; Bunz, U. H. F.; Srinivasarao, M. *J. Am. Chem. Soc.* **2006**, *128*, 7714–7715.
- (26) Furukawa, H.; Kim, J.; Ockwig, N. W.; O'Keeffe, M.; Yaghi, O. M. *J. Am. Chem. Soc.* **2008**, *130*, 11650–11661.
- (27) (a) Du, M.; Jiang, X.-J.; Zhao, X.-J. *Inorg. Chem.* **2006**, *45*, 3998–4006. (b) Du, M.; Jiang, X.-J.; Zhao, X.-J. *Inorg. Chem.* **2007**, *46*, 3984–3995.
- (28) SMART and SAINT. *Area Detector Control and Integration Software*; Siemens Analytical X-Ray Systems, Inc.: Madison, WI, 1996.
- (29) Sheldrick, G. M. *Acta Crystallogr.* **2008**, *A64*, 112–122.
- (30) Sheldrick, G. M. *SHELXL-97, Program for Crystal Structures Refinement*; University of Göttingen: Germany, 1997.
- (31) Bondi, A. *J. Phys. Chem.* **1964**, *68*, 441–451.
- (32) (a) Chen, X.-M.; Liu, G.-F. *Chem.—Eur. J.* **2002**, *8*, 4811–4817. (b) Zhang, L.-Y.; Liu, G.-F.; Zheng, S.-L.; Ye, B.-H.; Zhang, X.-M.; Chen, X.-M. *Eur. J. Inorg. Chem.* **2003**, 2965–2971.
- (33) Addison, A. W.; Rao, T. N. *J. Chem. Soc., Dalton Trans.* **1984**, 1349–1356.
- (34) LaDuca, R. L. *Coord. Chem. Rev.* **2009**, *253*, 1759–1792.
- (35) (a) Zhang, L.-Y.; Liu, G.-F.; Zheng, S.-L.; Ye, B.-H.; Zhang, X.-M.; Chen, X.-M. *Eur. J. Inorg. Chem.* **2003**, 2965–2971. (b) Hu, T.-L.; Zou, R.-Q.; Li, J.-R.; Bu, X.-H. *Dalton Trans.* **2008**, 1302–1311. (c) Ma, L.-F.; Wang, L.-Y.; Lu, D.-H.; Batten, S. R.; Wang, J.-G. *Cryst. Growth Des.* **2009**, *9*, 1741–1749. (d) Ma, L.-F.; Wang, L.-Y.; Wang, Y.-Y.; Batten, S. R.; Wang, J.-G. *Inorg. Chem.* **2009**, *48*, 915–924. (e) Zeng, M.-H.; Hu, S.; Chen, Q.; Xie, G.; Shuai, Q.; Gao, S.-L.; Tang, L.-Y. *Inorg. Chem.* **2009**, *48*, 7070–7079. (f) Ma, L.-F.; Wang, L.-Y.; Wang, Y.-Y.; Du, M.; Wang, J.-G. *CrystEngComm* **2009**, *11*, 109–117. (g) Ma, L.-F.; Wang, Y.-Y.; Liu, J.-Q.; Yang, G.-P.; Du, M.; Wang, L.-Y. *CrystEngComm* **2009**, *11*, 1800–1802. (h) Liu, D.; Li, H.-X.; Liu, L.-L.; Wang, H.-M.; Li, N.-Y.; Ren, Z.-G.; Lang, J.-P. *CrystEngComm* **2010**, *12*, 3708–3716.
- (36) (a) Batten, S. R. *CrystEngComm* **2001**, *3*, 67–73. (b) Carlucci, L.; Ciani, G.; Proserpio, D. M. *Coord. Chem. Rev.* **2003**, *246*, 247–289.
- (37) (a) Carlucci, L.; Ciani, G.; Proserpio, D. M. *CrystEngComm* **2003**, *5*, 269–279. (b) Baburin, I. A.; Blatov, V. A.; Carlucci, L.; Ciani, G.; Proserpio, D. M. *CrystEngComm* **2008**, *10*, 1822–1838. (c) Guo, H.-D.; Qiu, D.-F.; Guo, X.-M.; Batten, S. R.; Zhang, H.-J. *CrystEngComm* **2009**, *11*, 2611–2614. (d) Yao, Q.-X.; Ju, Z.-F.; Jin, X.-H.; Zhang, J. *Inorg. Chem.* **2009**, *48*, 1266–1268.
- (38) (a) Carlucci, L.; Ciani, G.; Proserpio, D. M.; Rizzato, S. *CrystEngComm* **2003**, *5*, 190–199. (b) Carlucci, L.; Ciani, G.; Maggini, S.; Proserpio, D. M. *Cryst. Growth Des.* **2008**, *8*, 162–165.
- (39) (a) Tao, J.; Zhang, X.-M.; Tong, M.-L.; Chen, X.-M. *J. Chem. Soc., Dalton Trans.* **2001**, 770–771. (b) Zhang, J.; Chew, E.; Chen, S.-M.; Pham, J. T. H.; Bu, X.-H. *Inorg. Chem.* **2008**, *47*, 3495–3497. (c) Li, M.-X.; Miao, Z.-X.; Shao, M.; Liang, S.-W.; Zhu, S.-R. *Inorg. Chem.* **2008**, *47*, 4481–4489.
- (40) (a) Tao, J.; Tong, M.-L.; Chen, X.-M. *J. Chem. Soc., Dalton Trans.* **2000**, 3669–3674. (b) Batten, S. R. *CrystEngComm* **2001**, *3*, 67–73. (c) Batten, S. R. Interpenetration. In *Encyclopedia of Supramolecular Chemistry*; Atwood, J. L.; Steed, J. W., Eds.; Marcel Dekker: New York, USA, 2004, 735–741. (d) Xiao, D.-R.; Li, Y.-G.; Wang, E.-B.; Fan, L.-L.; An, H.-Y.; Su, Z.-M.; Xu, L. *Inorg. Chem.* **2007**, *46*, 4158–4166. (e) Qi, Y.; Che, Y.-X.; Zheng, J.-M. *Cryst. Growth Des.* **2008**,

8, 3602–3608. (f) Wang, J.-J.; Liu, C.-S.; Hu, T.-L.; Chang, Z.; Li, C.-Y.; Yan, L.-F.; Chen, P.-Q.; Bu, X.-H.; Wu, Q.; Zhao, L.-J.; Wang, Z.; Zhang, X.-Z. *CrystEngComm* **2008**, *10*, 681–692. (g) Baburin, I. A.; Blatov, V. A.; Carlucci, L.; Ciani, G.; Proserpio, D. M. *CrystEngComm* **2008**, *10*, 1822–1838. (h) Yue, Q.; Qian, X.-B.; Yan, L.; Gao, E.-Q. *Inorg. Chem. Commun.* **2008**, *11*, 1067–1070. (i) Men, Y.-B.; Sun, J.; Huang, Z.-T.; Zheng, Q.-Y. *CrystEngComm* **2009**, *11*, 978–979. (j) Pigge, F. C.; Dighe, M. K.; Swenson, D. C. *CrystEngComm* **2009**, *11*, 1227–1230. (k) Li, Z.-X.; Xu, Y.; Zuo, Y.; Li, L.; Pan, Q.-H.; Hu, T.-L.; Bu, X.-H. *Cryst. Growth Des.* **2009**, *9*, 3904–3909. (l) Roy, S.; Mahata, G.; Biradha, K. *Cryst. Growth Des.* **2009**, *9*, 5006–5008. (m) Thakuria, R.; Sarma, B.; Nangia, A. *New J. Chem.* **2010**, *34*, 623–636.

(41) (a) Thaimattam, R.; Sharma, C. V. K.; Clearfield, A.; Desiraju, G. R. *Cryst. Growth Des.* **2001**, *1*, 103–106. (b) Liantonio, R.; Metrangolo, P.; Meyer, F.; Pilati, T.; Navarrini, W.; Resnati, G. *Chem. Commun.* **2006**, 1819–1821. (c) Metrangolo, P.; Meyer, F.; Pilati, T.; Proserpio, D. M.; Resnati, G. *Chem.—Eur. J.* **2007**, *13*, 5765–5772. (d) García, M. D.; Blanco, V.; Platas-Iglesias, C.; Peinador, C.; Quintela, J. M. *Cryst. Growth Des.* **2009**, *9*, 5009–5013.

(42) (a) Zhang, J.-P.; Lin, Y.-Y.; Huang, X.-C.; Chen, X.-M. *Eur. J. Inorg. Chem.* **2007**, 3407–3412. (b) Li, X.-J.; Cao, R.; Sun, D.-F.; Bi, W.-H.; Wang, Y.-Q.; Li, X.; Hong, M.-C. *Cryst. Growth Des.* **2004**, *4*, 775–780.

(43) Ma, C.-B.; Chen, C.-N.; Liu, Q.-T.; Chen, F.; Liao, D.-Z.; Li, L.-C.; Sun, L.-C. *Eur. J. Inorg. Chem.* **2004**, 3316–3325.

(44) Zhao, J.; Wang, X.-L.; Shi, X.; Yang, Q.-H.; Li, C. *Inorg. Chem.* **2011**, *50*, 3198–3205.

(45) (a) Bunz, U. H. F. *Chem. Rev.* **2000**, *100*, 1605–1644. (b) Frisch, M.; Cahill, C. L. *Dalton Trans.* **2005**, 1518–1523. (c) Yu, G.; Yin, S.; Liu, Y.; Shuai, Z.; Zhu, D. *J. Am. Chem. Soc.* **2003**, *125*, 14816–14824.